Omega-3 polyunsaturated fatty acids reverse the impact of western diets on regulatory T cell responses through averting ceramide-mediated pathways

Camacho-Muñoz, Dolores; Niven, Jennifer; Kucuk, Salih; Cucchi, Danilo; Certo, Michelangelo; Jones, Simon W; Fischer, Deborah P; Mauro, Claudio; Nicolaou, Anna

DOI:
10.1016/j.bcp.2022.115211

Document Version
Publisher's PDF, also known as Version of record

Citation for published version (Harvard):
Camacho-Muñoz, D, Niven, J, Kucuk, S, Cucchi, D, Certo, M, Jones, SW, Fischer, DP, Mauro, C & Nicolaou, A 2022, 'Omega-3 polyunsaturated fatty acids reverse the impact of western diets on regulatory T cell responses through averting ceramide-mediated pathways', *Biochemical Pharmacology*, vol. 204, 115211. https://doi.org/10.1016/j.bcp.2022.115211

Biochemical Pharmacology 204 (2022) 115211

Contents lists available at ScienceDirect

Biochemical Pharmacology

journal homepage: www.elsevier.com/locate/biochempharm

Omega-3 polyunsaturated fatty acids reverse the impact of western diets on regulatory T cell responses through averting ceramide-mediated pathways

Dolores Camacho-Muñoz [a,1], Jennifer Niven [b,1], Salih Kucuk [b,1], Danilo Cucchi [c], Michelangelo Certo [b], Simon W. Jones [b], Deborah P. Fischer [a], Claudio Mauro [b,c,*,2], Anna Nicolaou [a,d,2,*]

[a] Laboratory for Lipidomics and Lipid Biology, Division of Pharmacy and Optometry, School of Health Sciences, Faculty of Biology Medicine and Health, The University of Manchester, Manchester Academic Health Science Centre, Manchester M13 9PT, UK
[b] Institute of Inflammation and Ageing, College of Medical and Dental Sciences, University of Birmingham, Birmingham B15 2WB, UK
[c] William Harvey Research Institute, Barts and The London School of Medicine and Dentistry, Queen Mary University of London, London EC1M 6BQ, UK
[d] Lydia Becker Institute of Immunology and Inflammation, Faculty of Biology, Medicine and Health, The University of Manchester, Manchester Academic Health Science Centre, Manchester M13 9NT, UK

ARTICLE INFO

Keywords:
Ceramides
Regulatory T cells
High fat western diet
Omega 3 polyunsaturated fatty acids
Adipose tissue
Ceramide synthase

ABSTRACT

Western diet (WD), high in sugar and fat, promotes obesity and associated chronic low-grade pro-inflammatory environment, leading to impaired immune function, reprogramming of innate and adaptive immune cells, and development of chronic degenerative diseases, including cardiovascular disease. Increased concentrations of circulating and tissue ceramides contribute to inflammation and cellular dysfunction common in immune metabolic and cardiometabolic disease. Therefore, ceramide-lowering interventions have been considered as strategies to improve adipose tissue health.

Here, we report the ability of omega-3 polyunsaturated fatty acids (n-3PUFA) to attenuate inflammatory phenotypes promoted by WD, through ceramide-dependent pathways. Using an animal model, we show that enrichment of WD diet with n-3PUFA, reduced the expression of ceramide synthase 2 (CerS2), and lowered the concentration of long-chain ceramides (C23-C26) in plasma and adipose tissues. N-3PUFA also increased prevalence of the anti-inflammatory $CD4^+Foxp3^+$ and $CD4^+Foxp3^+CD25^+$ Treg subtypes in lymphoid organs. The CerS inhibitor FTY720 mirrored the effect of n-3PUFA. Treatment of animal and human T cells with ceramide C24 *in vitro*, reduced $CD4^+Foxp3^+$ Treg polarisation and IL-10 production, and increased IL-17, while it decreased Erk and Akt phosphorylation downstream of T cell antigen receptors (TCR). These findings suggest that molecular mechanisms mediating the adverse effect of ceramides on regulatory T lymphocytes, progress through reduced TCR signalling.

Our findings suggest that nutritional enrichment of WD with fish oil n-3PUFA can partially mitigate its detrimental effects, potentially improving the low-grade inflammation associated with immune metabolic disease. Compared to pharmacological interventions, n-3PUFA offer a simpler approach that can be accommodated as lifestyle choice.

1. Introduction

It is now widely recognised that western diet (WD), rich in high energy-dense foods, can promote non-communicable multifactorial disease, increasing the prevalence of obesity, immune metabolic conditions and cardiovascular disease (CVD) [1–4]. In particular, WD has been shown to foster a chronic low-grade pro-inflammatory environment associated with impaired immune function and reprogramming of

* Corresponding authors at: Institute of Inflammation and Ageing, College of Medical and Dental Sciences, University of Birmingham, Birmingham B15 2WB, UK (C. Mauro). Laboratory for Lipidomics and Lipid Biology, Division of Pharmacy and Optometry, School of Health Sciences, Faculty of Biology Medicine and Health, The University of Manchester, Manchester Academic Health Science Centre, Manchester M13 9PT, UK (A. Nicolaou).
E-mail addresses: c.mauro@bham.ac.uk (C. Mauro), anna.nicolaou@manchester.ac.uk (A. Nicolaou).
[1] Equal contribution; first authors.
[2] Equal contribution; senior authors.

https://doi.org/10.1016/j.bcp.2022.115211
Received 29 May 2022; Received in revised form 10 August 2022; Accepted 10 August 2022
Available online 17 August 2022

innate and adaptive immune cells, underpinning the development of chronic degenerative diseases, including CVD [1,3,5].

Regulatory T cells (Tregs) are a subset of $CD4^+$ T lymphocytes that express the transcription factor protein $Foxp3^+$ [6]. As well as being critical to controlling immune responses to self and environmental antigens, Tregs can promote tissue homeostasis and repair, and limit chronic inflammation [6–8]. The extensive phenotypic and functional diversity of Treg subtypes reflects their diverse origin and prevalence at different tissues, while their plasticity and function can be affected by diet components, including fatty acids [2,6,9,10]. Of importance to immune metabolic disease are the adipose tissue resident Tregs which interact with adipocytes and local immune cells, controlling the chronic low-grade inflammation associated with metabolic disorders, potentially, conferring protection [11–13]. WD can promote adipose tissue inflammation in a process driven by increased pro-inflammatory cell recruitment and insufficient anti-inflammatory responses of the resident Tregs [13–15]. It is therefore important to explore therapeutic approaches to combat the deleterious adipose tissue responses to WD, in order to maintain metabolic health.

Fatty acids mediate biological processes important for T lymphocytes, including their differentiation to specific T cell subsets and generation of immunological memory [9,16]. In particular, omega-3 (n-3) polyunsaturated fatty acids (PUFA) can suppress T cell antigen presentation, activation, proliferation and cytokine expression [10,17], while when used as nutritional supplements, they have shown promise in managing systemic inflammation [18]. Their protective activities are multifactorial, mediated through changes in cell membrane composition, gene expression, lipid mediator production and signalling cascades [10,17,19]. N-3PUFA can induce Treg differentiation via upregulation of peroxisome proliferator-activated receptor (PPAR) γ [20], reduce $CD4^+$ T cell activation *via* membrane raft related signalling [21,22], and as we have recently shown in a murine model, alter $CD4^+$ T cell migration through changes in cytoskeletal dynamics and membrane microdomains [23].

Ceramides are potent bioactive sphingolipid mediators involved in biological processes including cell proliferation, apoptosis, migration, senescence, autophagy and inflammation [24–26]. Ceramide biosynthesis and metabolism proceed through highly controlled reactions that belong to three pathways: the *de novo* biosynthesis, sphingomyelin storage and the salvage pathway. The *de novo* biosynthesis reactions are controlled by serine palmitoyl transferase (SPT) and progress through ceramide synthase (CerS) - a family of 6 isoforms (CerS1-6) that differ in substrate specificity and tissue distribution - to generate an array of ceramides, derivatives of sphingosine and other sphingoid bases, and fatty acids of varying lengths. Dysregulation in sphingolipid metabolism leads to increased concentrations of ceramides systemically and in tissues. Whereas circulating ceramides are considered biomarkers of CVD with increased heritability, tissue accumulation of ceramides can impair cellular function and metabolism [25,27–29]. Indeed, in adipose tissue, increased levels of ceramides are considered to contribute to inflammation and dysfunction underpinning the development to immune metabolic and cardiometabolic disease [25,26,29]. Ceramide-lowering interventions have been considered as effective strategies to improve adipose tissue health.

Here, we report the ability of n-3PUFA to attenuate inflammatory phenotypes promoted by WD, through ceramide-dependent pathways. Using an animal model, we show that enrichment of WD with n-3PUFA, reduced ceramide concentrations in plasma and adipose tissues, and promoted anti-inflammatory Treg subsets suppressed by ceramides through reduced TCR signalling. Our findings suggest that n-3PUFA intake can partially mitigate some of the detrimental effects of WD, potentially improving the low-grade inflammation associated with immune metabolic disease.

2. Materials and methods

2.1. Animal study

Animal experimentation took place in accordance with the UK Home Office regulations and was compliant with the European Parliament Directive 2010/63/EU for the protection of animals used in scientific research. Wild-type (WT) C57BL/6J female mice (5 weeks old, Charles River Laboratories, Bristol, UK) were allocated to groups of 6–7 animals each; they were fed either a chow diet (CD) (CRM-P, Special Diet Services, LBS Biotech, London, UK), a western diet (WD) (AIN-76A Western Diet, TestDiet, IPS, London, UK) or a western diet enriched with 5% menhaden oil (WD + ω3) (TestDiet® 5342, TestDiet, IPS, UK) for 21 days. The nutritional composition and fatty acid profile of all three diets are shown in Table 1. At the end of the study, no major changes in body parameters, including weight, were observed between the mice groups fed with either diet (mean body weight for CD: 19.0 ± 1.5 g; for WD: 18.7 ± 1.5 g; for WD + ω3: 19.0 ± 0.7 g). Immunisation took place 14 days after commencing the study (section 2.2). A further two groups of animals (6–7 animals each) were fed a WD for 21 days and treated with the ceramide synthase inhibitor FTY720 (SML0700-5MG; Merck, Gillingham, UK) [30] via 3 intraperitoneal injections (i.p.) (1 mg/kg) given

Table 1
(A) Composition of experimental chow diet (CD; CRM-P, SDS, UK), western diet (WD; AIN-76A, TestDiet, UK) and western diet enriched with omega-3 polyunsaturated fatty acids (n-3PUFA) using 5% menhaden oil (WD + ω3; TestDiet®5342, TestDiet UK). **(B)** Fatty acid composition of the menhaden fish oil used for the WD + ω3 diet. SFA: saturated fatty acids; MUFA: monounsaturated fatty acids; PUFA: polyunsaturated fatty acids.

A. **Composition of experimental diets**

Nutrients	**CD**	**WD**	**WD + ω3**
Energy (Kcal/g)	3.59	4.49	4.50
- Protein (%)	22.0	15.5	15.5
- Fat (%)	9.08	40.1	40.0
- Carbohydrates (%)	68.9	44.4	44.5
Sucrose (%)	3.90	34.0	34.3
Cholesterol (%)	–	0.15	0.15
Milk fat (%)	–	20.0	15.0
Corn oil (%)	–	1.00	0.70
Crude oil (%)	3.36	–	–
Menhaden oil (%)	–	–	5.00
Fatty Acid Composition (%)			
Linoleic acid (C18:2n-6)	0.96	1.07	0.84
α-Linolenic acid (C18:3n-3)	0.11	0.10	0.14
Arachidonic acid (C20:4n-6)	0.11	0.03	0.07
Total SFA	0.56	12.1	10.4
Total MUFA	0.99	4.61	4.48
Total n-3PUFA	0.11	0.21	1.51
Total PUFA	1.18	0.58	1.91

B. **Fatty acid profile of menhaden fish oil (%)**

Myristic Acid (C14:0)	6.85	Hexadecadienoic Acid (C16:2n-9)	1.62
Pentadecanoic Acid (C15:0)	0.46	Hexadecatrienoic Acid (C16:3n-6)	1.51
Palmitic Acid (C16:0)	14.8	Hexadecatetraenoic Acid (C16:4n-3)	1.53
Heptadecanoic Acid (C17:0)	0.38	Linoleic Acid (C18:2n-6)	1.93
Stearic Acid (C18:0)	2.55	α-Linolenic Acid (C18:3, n-3)	1.48
Arachidic Acid (C20:0)	0.17	Stearidonic Acid (C18:4n-3)	3.09
Behenic Acid (C22:0)	0.10	Auricolic Acid (C20:2n-3)	0.18
Lignoceric Acid (C24:0)	0.60	Bishomopinolenic Acid (C20:3n-6)	0.37
Total SFA	25.9	Arachidonic Acid (C20:4n-6)	2.09
Palmitoleic Acid (C16:1)	9.74	Eicosapentaenoic Acid (C20:5n-3)	14.2
Oleic Acid (C18:1)	9.58	Heneicosapentaenoic Acid (C21:5n-3)	0.76
Gadoleic Acid (C20:1)	1.48	Adrenic Acid (C22:4n-6)	0.24
Erucic Acid (C22:1)	0.33	Docosapentaenoic Acid (C22:5n-3)	2.82
Selacholeic Acid (C24:1)	0.22	Docosahexaenoic Acid (C22:6n-3)	12.2
Total MUFA	21.4	Total n-3 PUFA	36.3
		Total n-6 PUFA	6.14
		Total PUFA	44.0

at days 11, 16 and 18, or saline (vehicle control), as previously described [31,32]. These animals were also immunised at day 14 (section 2.2). At the end of the 21-day treatment period, all animals were sacrificed using CO_2 (Schedule 1 procedure).

2.2. In vivo T cell activation

In order to elicit an immune response and generate memory $CD4^+$ T cells, mice were subjected to allogenic immunisation as previously described [23]. In brief: at day 14 of the study the animals were given i.p. a mixture (1:1 ratio) of splenocytes from WT Balb/c and CBA male mice. After 7 days, the animals were sacrificed and mesenteric lymph nodes (mLN), spleen, adipose tissue from lower peritoneum (perigonadal fat) and subcutaneous fat, were harvested. Tissues used to isolate lymphocytes for flow cytometry analysis were processed fresh; tissues used for lipidomic analysis and RNA isolation were aliquoted, snap frozen and stored at −80 °C.

2.3. Murine in vitro $CD4^+$ T cell polarisation and treatment

Spleen and lymph nodes (mesenteric, inguinal and popliteal lymph nodes) were collected from naïve WT C57BL/6J female mice (n = 6 animals). Lymphocytes were harvested from tissue digests following treatment with 5% bovine serum albumin (BSA) containing collagenase Type II (Merck, UK) and washed with phosphate buffered saline (PBS) containing 2% foetal calf serum (FCS, Sera Laboratories International, London, UK), as described before [23]. $CD4^+$ T cells were isolated using the EasySepTM mouse $CD4^+$ T cell isolation kit (Stemcell Technologies, UK) according to the manufacturer's instructions. Cells were cultured in media consisting of RPMI-1640 (RO883, Merck, UK), 10% FCS, 1% non-essential amino acids, 1% penicillin and streptomycin, 1% L-glutamine and 0.1% beta-mercaptoethanol (β-ME). Murine $CD4^+$ T cells were activated with plate bound anti-CD3 (1 μg/mL, eBioscience, ThermoFisher Scientific, Horsham, UK), anti-CD28 (1 μg/mL, eBioscience, ThermoFisher Scientific, UK) and cultured for 3 days. Simultaneously with the activation, cells were also treated with ceramide C24 (d18:1/24:0, N(24)S(18)) (0.1 μM and 0.01 μM) (Avanti Polar Lipids, USA). Ceramide C24 was solubilised in a solution of methanol (VWR, Poole, UK) and fatty acid free BSA solution (4 mg BSA/ml of water, Merck, UK) (1:4, w/v), according to the supplier's instructions. The volume of C24 ceramide solutions used to treat the lymphocytes did not exceed 0.05% of the culture medium. Murine $CD4^+$ T cells were then polarised *in vitro*. For Th0, cells were treated with IL-2 (50 IU/ml); for Treg, cells were treated with IL-2 (50 IU/ml) (Peprotech, London, UK) and transforming growth factor beta (TGFβ) (10 ng/ml) (Biolegend, London, UK) [33]. Cells were then cultured for a further 3 days before being analysed by flow cytometry.

2.4. Human in vitro $CD4^+$ T cell polarisation and treatment

Human blood mononuclear cells (PBMC) were obtained from the Birmingham blood donor and transfusion centre (REC 20/WA/0092). $CD4^+$ T cells were isolated from PBMC using the Stemcell EasySepTM human naïve $CD4^+$T cell isolation Kit (Stemcell Technologies, Cambridge, UK) according to the manufacturer's instructions. The cells were then activated using human T cell activator beads (Dynabeads; ThermoFisher Scientific, UK) and treated with ceramide C24 (0.1 and 0.01 μM) as described in section 2.3. Human $CD4^+$ T cells were then polarised *in vitro*. For Th0, cells were treated with IL-2 (100 IU/ml); for Treg, cells were treated with IL-2 (100 IU/ml) (Peprotech, UK) and TGFβ (10 ng/ml) (Biolegend, UK) [33]. Cells were then cultured for a further 5 days before analysis by flow cytometry, while secreted cytokines were assessed by ELISA.

2.5. Flow cytometry

Lymphocytes were collected from animal lymphoid organs and fat tissues following digestion with 5% BSA containing collagenase Type II (Merck, UK) as described before [23]. Red blood cells present in the spleen samples were lysed before staining (Hybri-Max red blood cell lysis buffer, Merck, UK). Murine and human *ex vivo* polarised $CD4^+$ T cell subtypes were analysed after *in vitro* activation (described in sections 2.3 and 2.4 respectively). Dead cells were excluded from the analysis by staining with a live/dead stain (fixable Near IR Live and Dead; Invitrogen, UK). Surface staining of cell suspensions was performed using conjugated primary antibodies for the following markers: CD4 (RM4-5), CD44 (IM7), LFA1(M17/4), CXCR3 (CXCR3-173), BCL-2 (100) and CD25(PC61) (1:200, eBioscience, BioLegend, San Diego, USA). Antibodies were incubated at 4 °C for 30 min and washed in FACS buffer (2% FCS PBS). For intracellular staining, isolated cells were treated with a permeabilization buffer (eBioscience/Invitrogen), fixed and stained for Foxp3 (1:200, eBioscience, BioLegend, San Diego USA) at 4 °C for 30 min, as previously described [23]. Cell preparations were assessed by flow cytometry using an LSRFortessa (BD Biosciences, Berkshire, UK) and FlowJo software (version 10.7, BD Life Sciences, UK).

2.6. Cytokine analysis

The concentration of target cytokines (IL-10, IL-17A) in murine $CD4^+$ T cell culture supernatants was assessed using commercially available uncoated ELISA kits (Thermo Fisher Scientific, UK) according to the manufacturer's instructions. Briefly, 96-well flat-bottom high-affinity ELISA plates were coated overnight at 4 °C with the capture antibody and then treated with the blocking buffer before adding the test samples and standards. This was followed by successive incubation/wash steps with the detection antibody, (streptavidin-horseradish peroxidase) and assay substrate (tetramethylbenzidine) before incubating the final solutions in the dark. Optical density was measured using a microplate reader (Spectrostar omega; BMG Labtech, Aylesbury, UK) at 450–570 nm.

2.7. Western blotting

Human naïve $CD4^+$ T cells isolated from PBMC (described in section 2.4.) were treated with ceramide C24 (0.1 μM) overnight (12 h, 37 °C) and then activated using human T-cell activator beads (Dynabeads; ThermoFisher Scientific, UK) for 5, 10 and 15 min, or not activated. Then, cells were lysed in RIPA lysis buffer (Merck, UK) containing protease inhibitors (Merck, UK). The protein content of each sample was estimated using the Bradford assay (Bio-Rad, Watford, UK); equal amounts were separated by SDS PAGE (Mini-PROTEAN TGX Gels; Bio-Rad, Watford, UK) and transferred onto nitrocellulose membranes (Trans-Blot Turbo Transfer System and membranes; Bio-Rad, Watford, UK). Membranes were blocked at room temperature (1 h, using 5% Milk/TBS-T, Marvel, Merck, UK), incubated overnight at 4 °C with primary antibodies for phospho-Erk1/2 (Thr202/Tyr204), p44/42 MAPK (Erk1/2), phospho-Akt (Ser473) (D9E), Akt and β-actin (1:1000), followed by an anti-rabbit IgG, HRP-linked secondary antibody (1:2000) (all antibodies from Cell Signaling Technology, Danvers, Massachusetts, USA). Band densities were measured with ChemiDoc MP imaging system (Bio-Rad, UK) and processed using ImageJ software [34]. Protein band densities were normalised against the β-actin loading control, using the total of the two Erk or pErk bands according to the manufacturer's instructions; data shown as relative fold change (pAkt/Akt and pErk/Erk).

2.8. RNA isolation and quantitative real-time PCR

Total RNA was isolated from subcutaneous and perigonadal fat (≈20 mg tissue) using TRIzol reagent (Merck, UK) and purified using a

mirVana kit (Fisher Scientific, Loughborough, UK), according to the manufacturer's instructions. RNA quality and concentration was measured on a NanoDrop 2000 (Fisher Scientific, UK) before 1 μg was transcribed into cDNA using a QuantiTect Reverse Transcription kit (Qiagen, Manchester, UK). Quantitative real-time (qRT) cDNA amplification was performed in triplicate using SYBR Green Supermix (Qiagen, UK) and QuantiTect primer sets (GADPH (GeneGlobe ID QT01658692), Actb (GeneGlobe ID QT00095242), CerS2 (GeneGlobe ID QT00144025), CerS5 (GeneGlobe ID QT00101605) and CerS6 (GeneGlobe ID QT00137291)); Qiagen, UK) in a Quantstudio 12 K Flex RT-PCR system (Applied Biosystems, Waltham, Massachusetts, USA). Reactions conditions were: 50 °C for 2 min, 95 °C for 15 min and then 45 cycles of 94 °C for 15 s, 55 °C for 30 s, 72 °C for 30 s and cycle threshold (Ct) values were calculated. mRNA expression of CerS2, CerS5, CerS6 was normalized against the mean signal of β-actin and GAPDH housekeeping genes. Data were expressed as mean ± SEM relative to CD.

2.9. Ceramide UPLC/ESI-MS/MS analysis

Extraction and analysis of ceramides, phosphorylated ceramides, phosphorylated bases and free sphingoid bases was performed as described previously [23,28,35]. In brief, plasma (100–200 μl), perigonadal and subcutaneous fat tissue (30–40 mg) were homogenized in ice-cold chloroform/methanol (2:1, v/v, Fisher Scientific, UK), spiked with deuterated internal standards: 20 ng each of ceramide N(16)DS (18)-*d9*, ceramide N(18)S(18)-*d3* and ceramide A(16)S(18)-*d9* and 50 pmol of Cer/Sph Mixture I (Avanti Polar Lipids, USA). Following addition of ice-cold water (Fisher Scientific, UK), the organic layer was separated by centrifugation, evaporated to dryness and reconstituted in ethanol (Fisher Scientific, UK). Lipid extracts were analysed by ultrahigh performance liquid chromatography tandem mass spectrometry with an electrospray source (UPLC/ESI-MS/MS) using a Xevo-TQS mass spectrometer (Waters, Milford, Massachusetts, USA). Adipose tissue lipid extracts were cleaned-up by solid-phase extraction using a 100 mg Silica-Si cartridge (Strata SI-1-Silica; Phenomenex, UK) before analysed by UPLC/ESI-MS/MS. Ceramides were separated on a C8 column (Acquity UPLC BEH C8; 100 × 2.1 mm; 1.7 μm; Waters, USA) using a gradient elution with water and methanol, both modified with 0.1% formic acid (Fisher Scientific, UK). Detection was performed by multiple reaction monitoring (MRM) in the positive ionization mode; MRM transitions, indicative retention times and other experimental settings are provided in [35]. For instrument control and data acquisition MassLynx and TargetLynx software (Waters, USA) were used. Relative quantification of ceramides was carried out using the concentrations of deuterated and class specific internal standards. Proteins precipitated during lipid extractions were quantified using protein assay kit (Bio-Rad, Hemel Hempstead, UK), as described [36].

The notation used to describe ceramide species follows the system used by Masukawa *et al* [37,38]. For example, CER[NS] indicates a ceramide with a non-hydroxy fatty acid [N] and a sphingosine [S] base, whilst CER[NDS] is a ceramide with a non-hydroxy fatty acid [N] and a dihydro-sphingosine base [NS]. The acyl chain and sphingoid base carbon numbers for each ceramide species are shown in brackets (*e.g.,* N (24)S(18)) (Fig. 1**A**).

2.10. Statistical analysis

Statistical details of each experiment can be found in the figure legends. Statistical tests were selected based on appropriate assumptions with respect to data distribution and variance characteristics. Data distribution was assessed for normality using the Shapiro-Wilk and Kolmogorov-Smirnov tests. For the animal study, one-way ANOVA (uncorrected Fisher's LSD) was used to assess for differences in tissue ceramide concentrations between three groups and one-way ANOVA followed by Tukey's multiple comparisons post-hoc test was used to compare mRNA expression between three groups. For the cell studies, data were analysed by Mann-Whitney or one-tailed Student's *t*-test. Statistical analyses were performed using GraphPad Prism v.9 (GraphPad Software, San Diego, California, USA); a p-value of < 0.05 was considered to be statistically significant.

3. Results

3.1. N-3PUFA enrichment reverses WD-mediated increases in plasma and adipose tissue ceramides

Ceramide profiles of plasma, visceral (perigonadal) and peripheral (subcutaneous) fat tissues were analysed by UPLC/ESI-MS/MS to assess the impact of a diet high in saturated fatty acids, omega-6 (n-6) PUFA and refined sugar (WD), and the effect of enriching the WD with n-3PUFA (WD + ω3). We found a total of 50 ceramide species in the mouse tissues examined (Fig. 1**A**). CER[NS] and CER[NDS] were the main classes detected in both plasma and adipose tissues; the majority of these ceramides were derivatives of two 18 carbon (C18) sphingoid bases, namely sphingosine (S18) and dihydro-sphingosine (DS18) [37,38]. The most abundant ceramide species in all tissues examined were N(23)S (18) and N(24)S(18) (Fig. 1**A**). Lower concentrations of CER[NP], CER [AS] and CER[ADS] species were found in both adipose tissues and plasma, whereas some CER[AP] ceramides were detected in low abundance in perigonadal fat.

We observed that, in response to WD, the overall mean concentration of ceramides was increased in plasma, perigonadal fat and subcutaneous fat, compared to animals fed a CD diet (Fig. 1**B**) The impact of WD was greater on plasma ceramides, increasing the concentration of the most prevalent CER[NS] and CER[NDS] species, as well as the phosphorylated ceramide N(16)S(18) C1P (Fig. 1**A**). In the adipose tissues, WD significantly increased the most abundant CER[NS] species, notably N (23)S(18) and N(24)S(18) (Fig. 1**A**), as well as the sum of CER[NS] species (Fig. 1**B**), whereas CER[NDS] species were found either reduced (perigonadal fat) or not affected (subcutaneous fat). WD increased the fat tissue concentration of the phosphorylated ceramide N(16)S(18) C1P ($p < 0.0001$), similar to what was observed in plasma (Fig. 1**A**).

Interestingly, enrichment of the WD with n-3PUFA reduced both blood and fat tissue ceramides to basal (CD) levels (Fig. 1**A,B**). In plasma, n-3PUFA attenuated the effect of WD by reducing the concentration of almost all ceramides, while in the adipose tissues, n-3PUFA reduced CER[NS] but did not alter the levels of CER[NDS] species. Finally, the n-3PUFA enrichment increased adipose tissue levels of some minor CER[ADS] and CER[NP] species that had not been affected by WD.

3.2. N-3PUFA attenuate the WD-induced ceramide synthase gene expression in visceral fat

To understand the molecular mechanism underpinning the effect of the n-3PUFA enrichment of WD (WD + ω3 diet) on ceramide concentrations, we examined the molecular composition of ceramides found in plasma (systemic) and in adipose tissues (local). The majority of ceramides affected were CER[NS] derivatives of C18 sphingosine, with acyl chain lengths spanning from C14 to C28 (Fig. 2**A-C**). The WD diet significantly increased the concentration of ceramides with C23 and C24 acyl chains in both plasma and adipose tissues ($p < 0.0001$ and 0.05, respectively), and C26 ($p < 0.01$) in plasma, while the WD + ω3 diet attenuated this effect, reducing plasma and perigonadal fat ceramide concentration to control levels (Fig. 2**A,B**); the WD + ω3 diet did not have a significant effect on subcutaneous fat (Fig. 2**C**).

As the size of the sphingoid base was not affected, we examined the fat tissue expression of ceramide synthase (CerS), the enzyme determining the ceramide acyl chain length [39]. We measured gene expression of CerS2, CerS5 and CerS6, the isoforms that have specificity for C22-26, C14 and C16 acyl chains, respectively [39]. CerS2, CerS5 and CerS6 were found expressed in perigonadal and subcutaneous fat

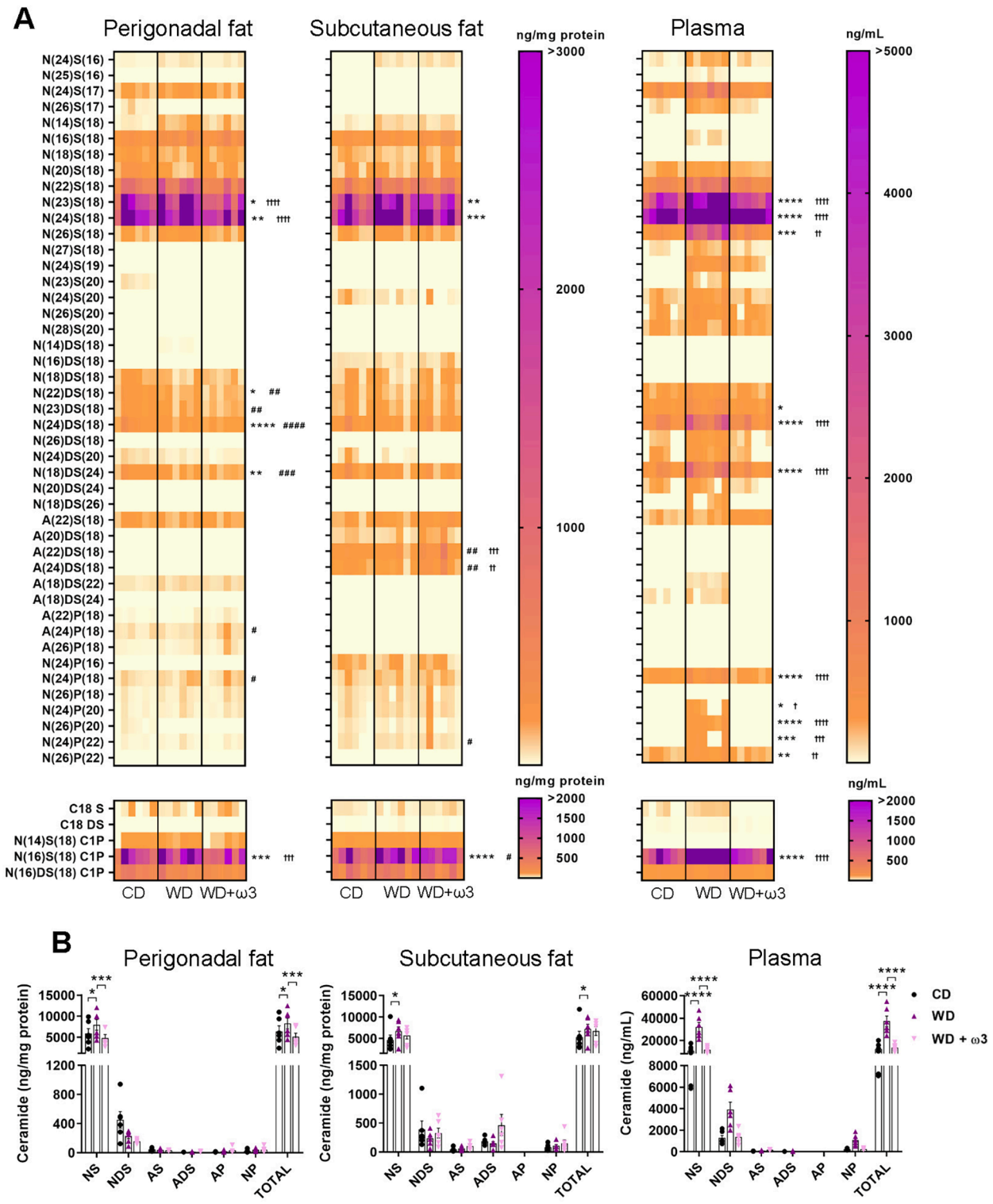

Fig. 1. Effect of western diet (WD) and n-3PUFA enriched WD (WD + ω3) on ceramides, sphingoid bases, phosphorylated ceramides found in fat tissues and plasma. As well as individual species (A), the WD and WD + ω3 diets altered ceramide classes and total ceramides (B). Tissue was obtained from female C57BL/6J WT mice fed a chow (CD), western (WD) or western with 5% menhaden oil (WD + ω3) diet (n = 6 mice per diet group). Data is expressed as ng/mg protein in solid tissues and ng/ml in plasma. The values denote individual values (A) or mean ± SEM (B); $^{*}p < 0.05$, $^{**}p < 0.01$, $^{***}p < 0.001$, $^{****}p < 0.0001$ comparing CD vs WD; $^{\#}p < 0.05$, $^{\#\#}p < 0.01$, $^{\#\#\#}p < 0.001$, $^{\#\#\#\#}p < 0.0001$ comparing CD vs WD + ω3; $^{\dagger}p < 0.05$, $^{\dagger\dagger}p < 0.01$. $^{\dagger\dagger\dagger}p < 0.001$, $^{\dagger\dagger\dagger\dagger}p < 0.0001$ comparing WD vs WD + ω3 (one-way ANOVA; uncorrected Fisher's LSD).

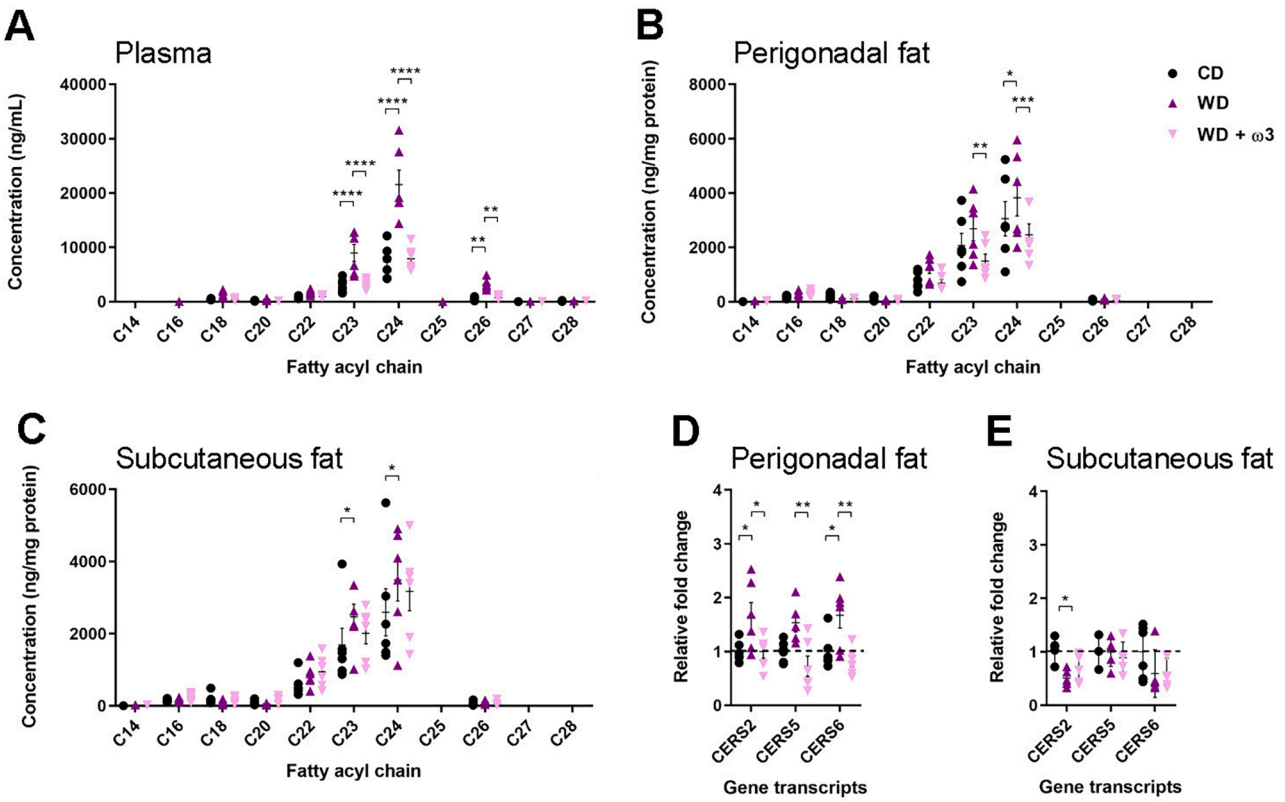

Fig. 2. Effect of western diet (WD) and n-3PUFA enriched WD (WD + ω3) on the fatty acyl chain of ceramides found in plasma (A), perigonadal fat (B) and subcutaneous fat tissue (C), and gene expression of CERS2, 5 and 6 in fat tissue (D, E). Tissue was obtained from female C57BL/6J WT mice fed a chow (CD), western (WD) or western with 5% menhaden oil (WD + ω3) diet (n = 6 mice per diet group). The values denote mean ± SEM (A-C). Data is expressed as ng/mg protein in solid tissues and ng/ml in plasma; *$p < 0.05$, **$p < 0.01$, ***$p < 0.001$, **** $p < 0.0001$ (one-way ANOVA; uncorrected Fisher's LSD). Ceramide synthase mRNA expression in perigonadal and subcutaneous fat in mice fed CD, WD or WD + ω3 (n = 6 animals per diet group). Total RNA was extracted using the TRIzol method, purified using a mirVana kit and quantified using qRT-PCR. Gene expression was normalized against β-actin and GAPDH and data were expressed as mean ± SEM relative to CD; *$p < 0.05$, **$p < 0.01$ (one-way ANOVA with Tukey's *post-hoc* adjustment).

(Fig. 2**D, E**). In perigonadal (visceral) fat, WD significantly increased CerS2, and S6 gene expression ($p < 0.05$ compared to CD); all changes were reversed following n-3PUFA enrichment of WD, and gene expression was reduced to control levels (Fig. 2**D,E**). Changes in subcutaneous fat CerS gene expression were less profound, and CerS2 expression decreased following WD ($p < 0.05$ WD vs control).

3.3. N-3PUFA enrichment increases anti-inflammatory CD4$^+$Foxp3$^+$ Treg subtypes in perigonadal fat-draining lymphoid tissues of WD-fed animals

As n-3PUFA enrichment of WD was found to reduce ceramide levels systemically (plasma) and locally (adipose tissue), we examined whether this effect was accompanied by changes in T cell profiles in lymphoid organs and fat tissues. The numbers and subtypes of CD4$^+$ T cells present in spleen, mLN and perigonadal fat were assessed by flow cytometry. Dietary enrichment with n-3PUFA led to a significant increase of CD4$^+$Foxp3$^+$ Tregs in the spleen and mLNs of the WD + ω3 animals compared to WD (Fig. 3**A**); a similar trend was observed in perigonadal fat, although did not reach statistical significance. Increased prevalence of the anti-inflammatory CD4$^+$Foxp3$^+$CD25$^+$ Tregs, typically found in peripheral tissues [6], was also significantly increased in the spleen, but not mLN or perigonadal fat of WD + ω3-fed animals (Fig. 3**B**). The impact of WD + ω3 was restricted to Tregs as we did not observe any significant changes in the prevalence of the pro-inflammatory effector memory CD44$^+$LFA1$^+$ and CD44$^+$CXCR3$^+$ T cell subtypes, known to infiltrate inflammatory tissues (Fig. 3**C and D**, respectively) [40].

3.4. Inhibition of CerS increases prevalence of CD4$^+$Foxp3$^+$ Treg subtypes in lymphoid tissues of WD-fed animals

To confirm whether the observed changes in Tregs were a consequence of n-3PUFA-induced inhibition of ceramides through reduced expression of CerS, mice fed a WD were systemically treated with FTY720, a widely used non-specific CerS inhibitor [31,32,41,42]. Analysis of plasma samples showed that FTY720 inhibited total plasma ceramides ($p < 0.01$), also reducing the concentration of species produced by CerS2 (C22-26), including C24 (Fig. 4**A**).

Flow cytometry analysis showed that the FTY720-treated animals had significantly higher numbers CD4$^+$Foxp3$^+$ Treg in both spleen and mLN, compared to untreated WD-fed animals; this change was accompanied by concomitant lower proportion of CD4$^+$Foxp3$^-$ Tregs (Fig. 4**B**). Additionally, inhibition of CerS led to a significant increase in the anti-inflammatory CD4$^+$Foxp3$^+$CD25$^+$ Treg population with increased incidence of Foxp3$^+$BCL2$^+$ cells in both spleen and mLN (Fig. 4**C and D**, respectively) suggesting activation of anti-apoptotic pathways by FTY720 [43]. The effect of FTY720 was similar to that observed following the n-3PUFA intervention.

3.5. Ceramides interfere with Treg differentiation and cytokine production

To obtain mechanistic insights and elucidate the role of ceramides in Treg cell biology, isolated murine CD4$^+$ T lymphocytes were differentiated to Treg *ex vivo* (Fig. 5**A**) in the presence of the long chain ceramide N(24)S(18) (C24). We studied the impact of C24 ceramide, as this was

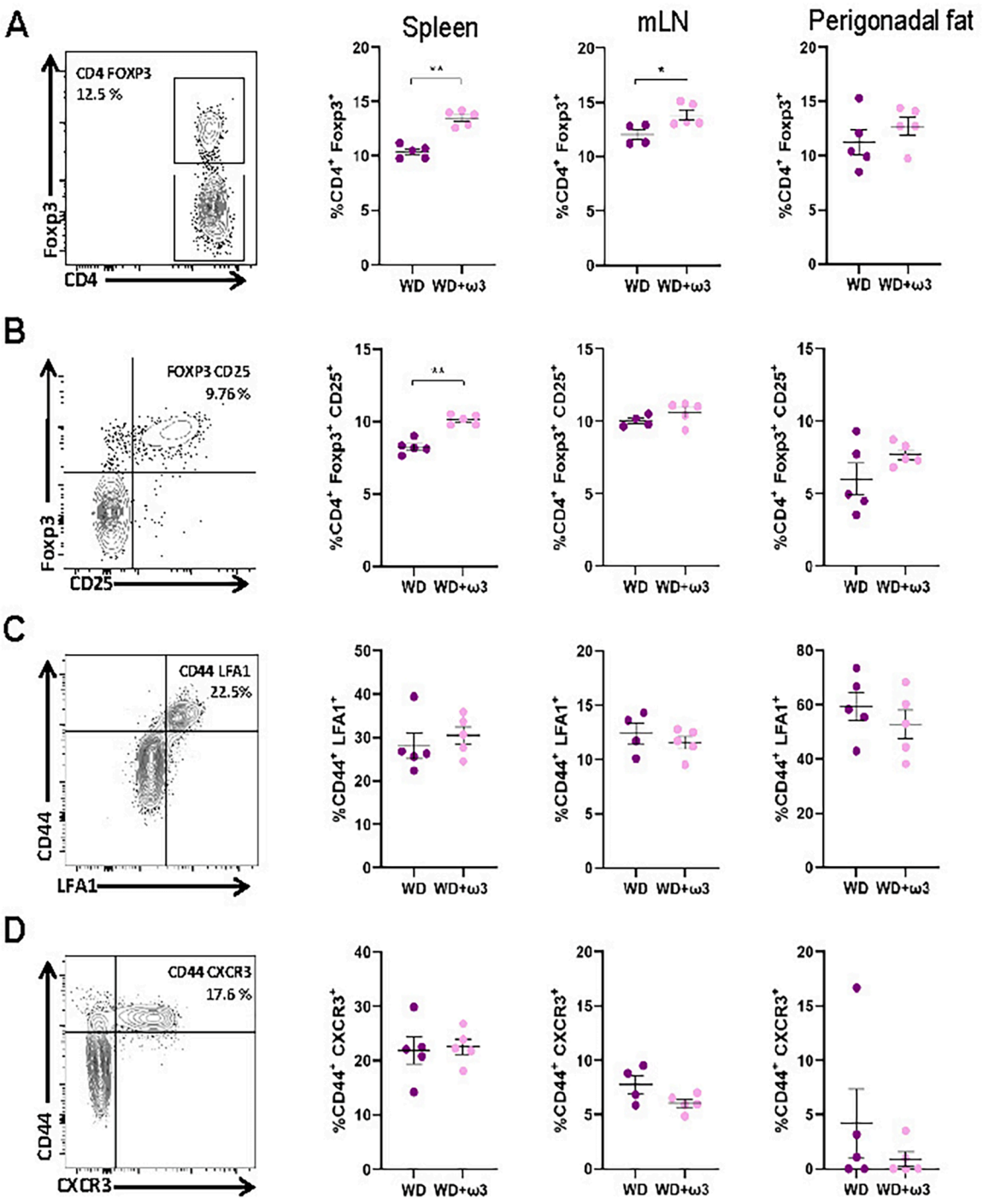

Fig. 3. N-3PUFA enrichment of WD alters the distribution of T cell subsets in lymphoid organs and fat tissue. Female C57BL/6J mice (n = 4–5) were fed western (WD) or western with 5% menhaden oil (WD + ω3) for 21 days and were subjected to an allogenic immunization via intraperitoneal injections at day 14. Data is expressed as mean of frequency of $Foxp3^+$ (A) and $Foxp3^+$ $CD25^+$ (B), within the total live $CD4^+$ T cell population, and $LFA1^+$ (C) and $CXCR3^+$ within the total live $CD44^+$ T cell population, in the spleen, mesenteric lymph node (mLN) and perigonadal fat. Representative FACS plot showing the gating (A, B, C, D). Data is expressed as mean ± SEM; *$p < 0.05$; **$p < 0.01$ (Mann-Whitney test).

the most abundant species identified in the animal study (Fig. 1**A**), it was reduced following n-3PUFA dietary intervention, and was also commercially available as synthetic standard. Ceramide C24 was assessed at concentrations found in the animal tissues (Fig. 1).

Differentiation of murine $CD4^+$ T lymphocytes in the presence of ceramide C24 (0.1 μM, 3 days) showed significant reduction of $CD4^+Foxp3^+$ Tregs compared to untreated control cells ($p < 0.01$) (Fig. 5**B**). A concomitant reduction in IL-10 production ($p < 0.05$), a cytokine produced by $CD4^+Foxp3^+$ Tregs, confirmed the effect of C24 in reducing the prevalence of this T cell subtype (Fig. 5**C**). Treatment with C24 (0.1 μM, 3 days) resulted in a significant increase in IL-17 production ($p < 0.01$) (Fig. 5**D**), suggesting a shift towards an inflammatory phenotype. The treatment had no effect on the prevalence of $CD4^+INF\gamma^+$ T cells (Fig. 5**E**). Ceramide C24 treatment did not induce murine T cell toxicity, and all groups had > 80% cell viability as assessed by flow cytometry (Fig. 5**F**).

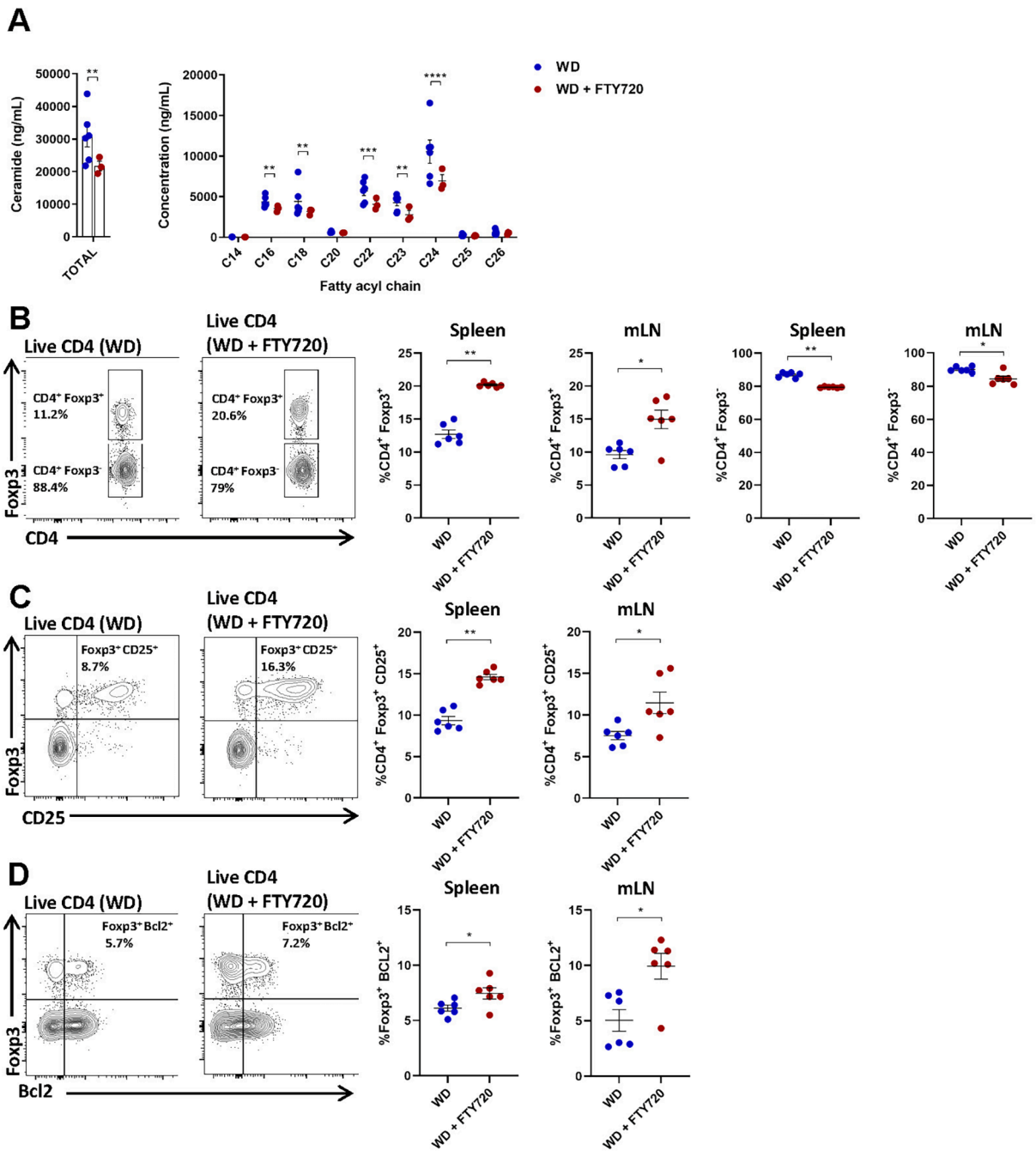

Fig. 4. The ceramide synthase (CerS) inhibitor FTY720 reduces plasma ceramides (A), and increases Foxp3$^+$ (B), Foxp3$^+$ CD25$^+$ (C) and Foxp3$^+$ BCL2$^+$ (D) Tregs in lymphoid tissues. Total plasma ceramide concentrations and distribution of fatty acyl chain of ceramides (A). Representative FACS plots showing the gating of Foxp3$^+$ (B), Foxp3$^+$ CD25$^+$ (C) and Foxp3$^+$ BCL2$^+$ (D) regulatory T cells (Tregs). Female C57BL/6J mice (n = 6) were fed western diet (WD) for 21 days and were subjected to an allogenic immunization via intraperitoneal injections at day 14. Inhibition group mice were given intraperitoneal injections of FTY720 (1 mg/kg) or vehicle control three times (days 11, 14 and 18) (WD + FTY720). Ceramide data expressed as ng/ml in plasma, mean ± SEM; $^{**}p < 0.01$, $^{***}p < 0.001$, $^{****}p < 0.0001$ (one-way ANOVA; uncorrected Fisher's LSD). T cell data expressed mean of frequency ± SEM of Foxp3$^+$ and Foxp3$^-$ (B), Foxp3$^+$ CD25$^+$ (C) and Foxp3$^+$ BCL2$^+$ Tregs (D) within the total live CD4$^+$ T cell population in the spleen and mesenteric lymph node (mLN); $^{*}p < 0.05$; $^{**}p < 0.01$ (Mann-Whitney test).

3.6. Ceramides reduce Treg differentiation via Akt and Erk downstream of TCR signalling

As treatment with ceramide C24 appeared to divert the differentiation of Tregs towards an inflammatory Th17 phenotype, we explored its effect on Akt and Erk phosphorylation. These signalling pathways are downstream of the TCR and their activation can be used as proxy of the strength of the TCR signal [44]. The experimental design requires the overnight conditioning of T cells with ceramide C24 before triggering CD3/CD28 expression leading to TCR activation. However, naïve murine T cells are not viable in culture unless their TCR is engaged immediately after purification [45], hence the Akt and Erk experiments were performed with human naïve CD4$^+$ T cells isolated from PBMCs, which are in a state of pre-activation and can be cultured for a few hours without TCR triggering.

Human naïve CD4$^+$ T lymphocytes isolated from PBMCs, were treated with ceramide C24 (0.1 μM, 5 days) and polarised *in vitro*. The C24 treatment reduced CD4$^+$Foxp3$^+$ Treg differentiation ($p < 0.01$)

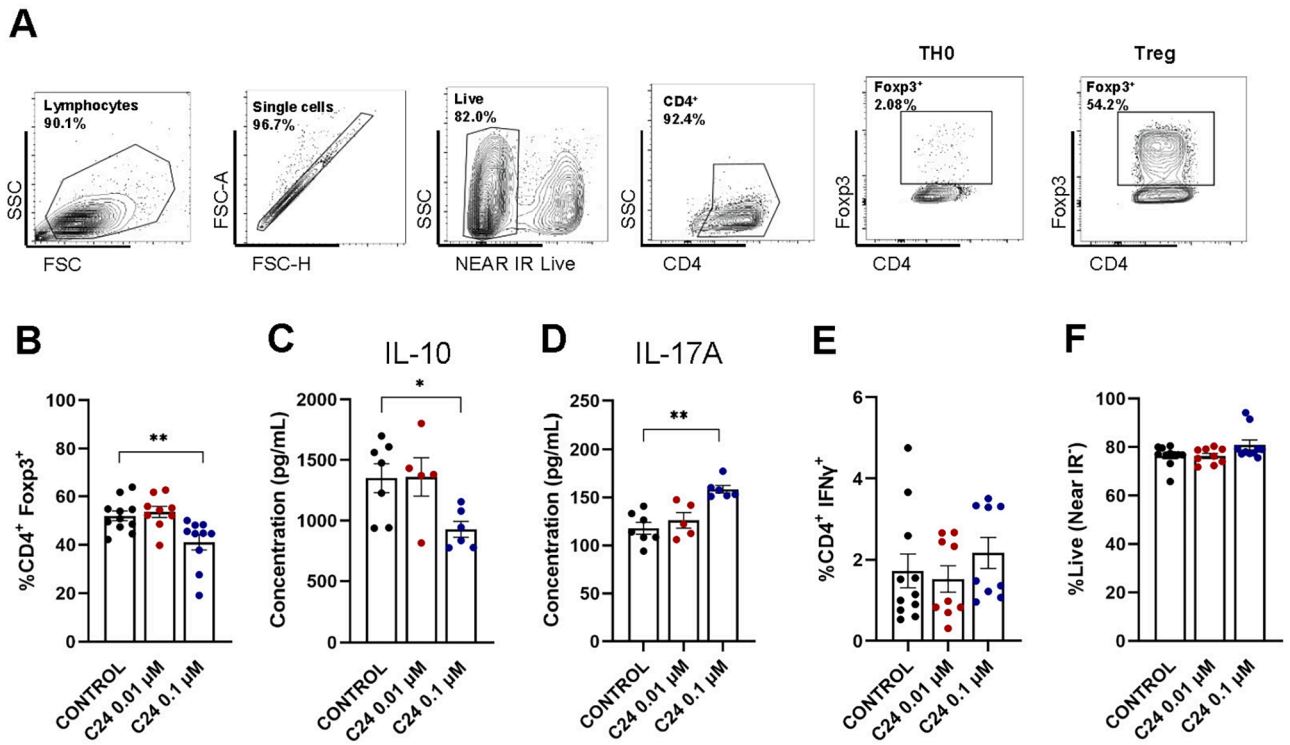

Fig. 5. C24 ceramide reduces Foxp3$^+$ Treg differentiation (A) and production of IL-10 (B), increases production of IL-17A (C), but does not alter the prevalence of CD4$^+$IFNγ$^+$ T cells (D) or cell viability (E) in an animal model. Pooled CD4$^+$ T cells (n = 5–6 mice) were treated with C24 ceramide (0.01 and 0.1 μM) or left untreated for 3 days, followed by CD3/CD28 (1 μg/mL) plate bound activation, *in vitro*. Data expressed as mean of frequency ± SEM of Foxp3$^+$ (A), mean concentration ± SEM of IL-10 (B) and IL-17 (C), mean frequency ± SEM of INF$^+$, and mean ± SEM of live cell numbers (E); *$p < 0.05$; **$p < 0.01$ (Mann-Whitney test). Representative flow cytometry gating strategy used *in vitro* CD4$^+$ T cell differentiation assay. Lymphocytes were gated according to their typical location on forward and side scatter followed by live CD4$^+$ singlets and Th0 (control group) and regulatory T cells gated according to Foxp3 marker (F).

(Fig. 6**A**), without affecting cell viability (Fig. 6**C**). Following CD3/CD28 activation of the ceramide C24-treated CD4$^+$ T cells (0.1 μM), a reduction in pAkt and pErk (Fig. 6**B**) expression was observed; the effect was noted as early as 10 min for pAkt ($p < 0.05$) and 5 min for pErk ($p < 0.05$).

4. Discussion

Our results show that, in an animal model, enrichment of WD with n-3PUFA-containing fish oil reduces the expression of CerS2 and the concentration of long-chain ceramides (C23-C26) in plasma and adipose tissues, and it increases the prevalence of the anti-inflammatory CD4$^+$Foxp3$^+$ and CD4$^+$Foxp3$^+$CD25$^+$ Treg subtypes in lymphoid organs. Pharmacological use of the CerS inhibitor FTY720 in WD-fed animals, mirrored the effect of the n-3PUFA intervention, supporting the notion that ceramide-mediated pathways underpin the observed Treg differentiation. Ceramide C24, the most abundant species found in the animal tissues, reduced CD4$^+$Foxp3$^+$ Treg polarisation and IL-10 production *ex vivo*, and decreased Erk and Akt phosphorylation in ceramide C24-treated Tregs. These findings suggest that aspects of the molecular mechanism mediating the adverse effect of ceramides on CD4$^+$ T cells, progress through reduced TCR signalling.

Diets high in fat, such as the WD, stimulate ceramides with consequent promotion of inflammatory and pro-apoptotic pathways, while saturated fatty acids such as palmitate, typically high in WD, advance ceramide lipotoxicity [26,46–49]. Dysregulated sphingolipid metabolism is also implicated in several immune metabolic diseases, with increased level of blood ceramides now considered as a CVD biomarker [27,29]. Furthermore, pharmacological inhibition, genetic modifications, and KO models of CerS have demonstrated that reducing liver, adipose tissue and plasma ceramides improves systemic health [50–53]. Reducing ceramides is also beneficial for T cells as it leads to higher TCR signal and increased prevalence of Tregs, potentially conferring protection and reducing inflammation [54,55].

Reducing ceramides via WD enrichment with fish oil n-3PUFA or CerS inhibition, increased the anti-inflammatory CD4$^+$Foxp3$^+$ and CD4$^+$Foxp3$^+$CD25$^+$ Treg subtypes. CD4$^+$Foxp3$^+$CD25$^+$ Tregs found mainly in the blood, may promote disease resolution, and can protect against atherogenesis [56]. Furthermore, the CerS inhibitor significantly increased the expression of BCL2$^+$, a marker of enhanced Treg differentiation and immunosuppression [43]. Interestingly, in our model, inhibition of ceramides did not reduce other proinflammatory cell types. This finding suggests a specificity towards Tregs that needs to be further explored and confirmed, as ceramides are important for the differentiation and effector function of CD4$^+$ T lymphocytes, and their levels may impact upon the prevalence of other T cell subtypes [57].

In search of the molecular mechanism underpinning the activity of ceramides, we showed that C24 diverted Treg differentiation from an IL-10, immunosuppressive phenotype towards a pro-inflammatory Th17 phenotype. Our data also suggests that C24 ceramide can reduce the strength of the TCR signal, as indicated by reduced downstream Akt and Erk phosphorylation [44,58,59]. The frequency of Tregs expressing IL-17 is increased in patients with immune mediated chronic disease such as psoriasis, inflammatory bowel disease and rheumatoid arthritis [44]. However, we did not notice an increase in IFN-γ-producing Tregs, typically associated with autoimmune disease [44].

In our study, the impact of inhibiting ceramides affected mainly the lymphoid organ Tregs. This could be attributed to the experimental design as the animals were fed the WD or WD + ω3 diets for only 3 weeks, and they were not obese. Further work using higher n-3PUFA doses, longer supplementation periods, with obese or older animals, or models of immune metabolic disease are needed to explore the

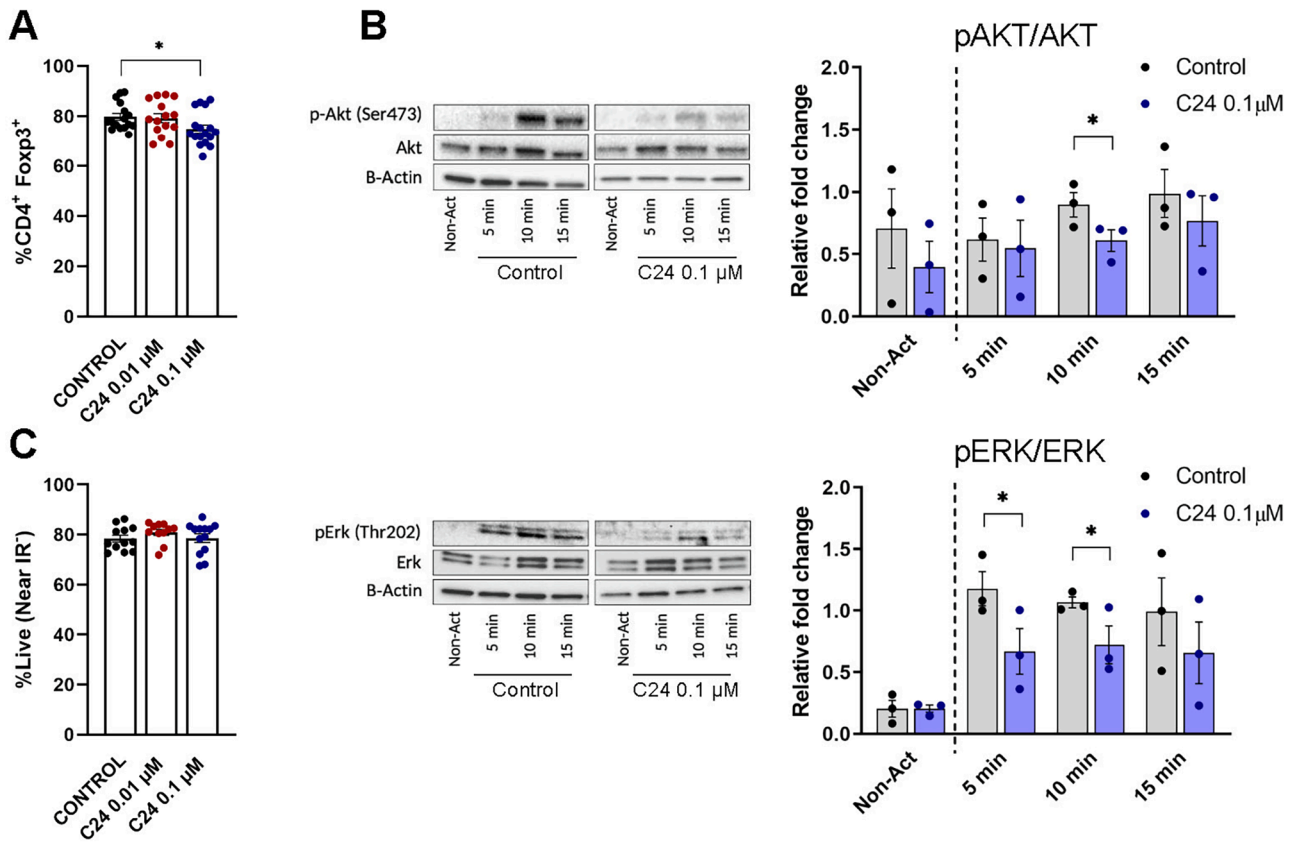

Fig. 6. C24 ceramide reduces Foxp3$^+$ Treg differentiation (A) and TCR signalling (B) in a human model. CD4$^+$ T cells isolated from human PBMCs (n = 4 donors) were treated with C24 ceramide (0.01 and 0.1 µM) or left untreated for 5 days. Human dynabeads T cell activator (CD3/CD28) kit (bead-to-cell ratio of 1:1) used for T cell activation. Data expressed as mean of frequency ± SEM of Foxp3$^+$(A) and mean ± SEM of live cell numbers (C). Representative western blots and densitometric quantification of pAkt, Akt, pErk and Erk expression (B); data expressed as mean ± SEM relative to Akt and Erk; *$p < 0.05$ (one-tailed Student's *t*-test).

efficiency of the supplement. Adipose tissue resident CD4$^+$Foxp3$^+$ Treg are important in establishing peripheral tolerance and may be protective [8,12]. It is therefore important to examine whether adipose-specific Treg lineages are responding similarly to T cells differentiated in the lymphoid organs prior to entering the circulation to reach peripheral inflamed tissues [6,12,13].

Our findings clearly show that when the WD is enriched with fish oil n-3PUFA, it can significantly reduce a range of ceramide species including the commonly examined CER[NS], but also the dihydrosphingosine CER[NDS] species, an emerging target for metabolic disease [60]. Our study demonstrates that the impact of n-3PUFA is more profound in plasma ceramides, suggesting a systemic effect with impact on multiple tissues including the liver, a major site for ceramide production. Ceramide synthases CerS2, CerS5 and CerS6 are highly expressed in the adipose tissue and liver, having been linked to glucose homeostasis and insulin resistance [39,49]. Our data show that visceral but not subcutaneous fat had a more profound response to WD and n-3PUFA enrichment of WD, both in terms of ceramide production and Treg differentiation. Inflamed visceral fat is involved in obesity and immune metabolic disease, therefore local ceramide production may be important for both resident and infiltrating T lymphocytes. As both CD and WD animal diets contained adequate amounts of the essential n-3PUFA α-linolenic acid (ALA; C18:3n-3) (Table 1), the beneficial effects reported here can be directly attributed to eicosapentaenoic (EPA; C20:5n-3), docosahexaenoic (DHA; C22:6n-3), docosapentaenoic (DPA; C22:5n-3), stearidonic acid (C18:4n-3) and other n-3PUFA species found in the fish oil used to enrich the WD diet. Whether the beneficial activity of fish oil is attributed to its individual n-3PUFA components or their mixtures remains to be explored.

Compared to pharmacological interventions, nutritional supplementation with n-3PUFA can offer a simpler, more affordable intervention to alleviate and, potentially, reverse the detrimental effects of WD. As the effect of n-3PUFA occurs without the requirement to stop the WD, it has the additional advantage of being accommodated as a lifestyle change. Further work should explore the effectiveness of this approach in disease; in a recent study with non-alcoholic fatty liver disease (NAFLD) patients, n-3PUFA were less effective in reducing plasma ceramides compared to fenofibrate [35]. This may be an overall limitation of the nutritional supplementation approach as it may not be effective in reversing ceramide pathways after the onset of disease. However, it could be used to counteract the early stages of damage caused by high fat diets, controlling ceramide production, and acting as a prevention strategy.

Overall, n-3-PUFA enrichment of WD appears to act as ceramide production inhibitor, attenuating the negative effects of a diet high in fat, and in doing so, improve the profile and population of immune cells, potentially ameliorating overall health. Fish oil n-3PUFA are safer than pharmacological agents and can be taken as supplements but also through foods, without the need for expensive interventions.

CRediT authorship contribution statement

Dolores Camacho-Muñoz: Writing – original draft, Investigation, Methodology, Formal analysis, Visualization. **Jennifer Niven:** Writing – review & editing, Investigation, Methodology, Formal analysis. **Salih Kucuk:** Writing – review & editing, Investigation, Formal analysis. **Danilo Cucchi:** Investigation. **Michelangelo Certo:** Visualization, Investigation, Formal analysis, Writing – review & editing. **Simon W. Jones:** Supervision, Writing – review & editing. **Deborah P. Fischer:** Investigation, Writing – review & editing. **Claudio Mauro:** Funding

acquisition, Project administration, Supervision, Writing – review & editing, Conceptualization. **Anna Nicolaou:** Funding acquisition, Project administration, Supervision, Conceptualization, Writing – original draft.

Declaration of Competing Interest

The authors declare that they have no known competing financial interests or personal relationships that could have appeared to influence the work reported in this paper.

Acknowledgements

The work has been supported by a grant from the British Heart Foundation (PG/15/105/31906) to A.N. and C.M. C.M. is supported by a British Heart Foundation Intermediate Basic Science Research Fellowship (FS/12/38/29640) and a Professorial Fellowship from the University of Birmingham. The authors wish to thank Neil O'Hara (University of Manchester) for excellent technical support and Dr Jorge Caamano (University of Birmingham) for support in experimental design and intellectual contribution.

References

[1] A. Christ, M. Lauterbach, E. Latz, Western Diet and the Immune System: An Inflammatory Connection, Immunity 51 (5) (2019) 794–811, https://doi.org/10.1016/j.immuni.2019.09.020.
[2] R. Arroyo Hornero, I. Hamad, B. Côrte-Real, M. Kleinewietfeld, The Impact of Dietary Components on Regulatory T Cells and Disease, Front. Immunol. 11 (2020) 253, https://doi.org/10.3389/fimmu.2020.00253.
[3] C. García-Montero, O. Fraile-Martínez, A.M. Gómez-Lahoz, L. Pekarek, A. J. Castellanos, F. Noguerales-Fraguas, S. Coca, L.G. Guijarro, N. García-Honduvilla, A. Asúnsolo, L. Sanchez-Trujillo, G. Lahera, J. Bujan, J. Monserrat, M. Álvarez-Mon, M.A. Álvarez-Mon, M.A. Ortega, Nutritional Components in Western Diet Versus Mediterranean Diet at the Gut Microbiota-Immune System Interplay. Implications for Health and Disease, Nutrients 13 (2) (2021) 699, https://doi.org/10.3390/nu13020699.
[4] A. Manzel, D.N. Muller, D.A. Hafler, S.E. Erdman, R.A. Linker, M. Kleinewietfeld, Role of "Western diet" in inflammatory autoimmune diseases, Curr. Allergy Asthma Rep. 14 (1) (2014) 404, https://doi.org/10.1007/s11882-013-0404-6.
[5] S. Kucuk, J. Niven, J. Caamano, S.W. Jones, D. Camacho-Muñoz, A. Nicolaou, C. Mauro, Unwrapping the mechanisms of ceramide and fatty acid-initiated signals leading to immune-inflammatory responses in obesity, Int. J. Biochem. Cell Biol. 135 (2021) 105972, https://doi.org/10.1016/j.biocel.2021.105972.
[6] L.E. Sjaastad, D.L. Owen, S.I. Tracy, M.A. Farrar, Phenotypic and Functional Diversity in Regulatory T Cells, Front. Cell Dev. Biol. 9 (2021) 715901, https://doi.org/10.3389/fcell.2021.715901.
[7] P. Pandiyan, J. Zhu, Origin and functions of pro-inflammatory cytokine producing Foxp3^{+} regulatory T cells, Cytokine 76 (1) (2015) 13–24, https://doi.org/10.1016/j.cyto.2015.07.005.
[8] A. Sharma, D. Rudra, Emerging Functions of Regulatory T Cells in Tissue Homeostasis, Front. Immunol. 9 (2018) 883, https://doi.org/10.3389/fimmu.2018.00883.
[9] D. Cucchi, D. Camacho-Muñoz, M. Certo, V. Pucino, A. Nicolaou, C. Mauro, Fatty acids - from energy substrates to key regulators of cell survival, proliferation and effector function, Cell Stress 4 (1) (2019) 9–23, https://doi.org/10.15698/cst2020.01.209.
[10] S. Gutiérrez, S.L. Svahn, M.E. Johansson, Effects of Omega-3 Fatty Acids on Immune Cells, Int. J. Mol. Sci. 20 (20) (2019) 5028, https://doi.org/10.3390/ijms20205028.
[11] X. Chen, Y. Wu, L. Wang, Fat-resident Tregs: an emerging guard protecting from obesity-associated metabolic disorders, Obes. Rev. 14 (7) (2013) 568–578, https://doi.org/10.1111/obr.12033.
[12] D. Cipolletta, Adipose tissue-resident regulatory T cells: phenotypic specialization, functions and therapeutic potential, Immunology 142 (4) (2014) 517–525, https://doi.org/10.1111/imm.12262.
[13] P. Sivasami, C. Li, Derivation and Differentiation of Adipose-Tissue Regulatory T Cells: A Stepwise, Multi-Site Process, Front. Immunol. 11 (2020) 599277, https://doi.org/10.3389/fimmu.2020.599277.
[14] A. Sakers, M.K. De Siqueira, P. Seale, C.J. Villanueva, Adipose-tissue plasticity in health and disease, Cell 185 (3) (2022) 419–446, https://doi.org/10.1016/j.cell.2021.12.016.
[15] E. Fuentes, F. Fuentes, G. Vilahur, L. Badimon, I. Palomo, Mechanisms of Chronic State of Inflammation as Mediators That Link Obese Adipose Tissue and Metabolic Syndrome, Mediators Inflamm. 2013 (2013) 136584. DOI: 10.1155/2013/136584.
[16] A. Nicolaou, C. Mauro, P. Urquhart, F. Marelli-Berg, Polyunsaturated Fatty Acid-derived lipid mediators and T cell function, Front. Immunol. 5 (2014) 75, https://doi.org/10.3389/fimmu.2014.00075.
[17] S.R. Shaikh, M. Edidin, Immunosuppressive effects of polyunsaturated fatty acids on antigen presentation by human leukocyte antigen class I molecules, J. Lipid Res. 48 (1) (2007) 127–138, https://doi.org/10.1194/jlr.M600365-JLR200.
[18] P.C. Calder, n-3 PUFA and inflammation: from membrane to nucleus and from bench to bedside, Proc. Nutr. Soc. 79 (4) (2020) 404–416, https://doi.org/10.1017/s0029665120007077.
[19] P.C. Calder, The relationship between the fatty acid composition of immune cells and their function, Prostaglandins Leukot. Essent. Fatty Acids 79 (3) (2008) 101–108, https://doi.org/10.1016/j.plefa.2008.09.016.
[20] D. Iwami, Q. Zhang, O. Aramaki, K. Nonomura, N. Shirasugi, M. Niimi, Purified Eicosapentaenoic Acid Induces Prolonged Survival of Cardiac Allografts and Generates Regulatory T Cells, Am. J. Transplant. 9 (6) (2009) 1294–1307, https://doi.org/10.1111/j.1600-6143.2009.02641.x.
[21] S.R. Shaikh, H. Teague, N-3 fatty acids and membrane microdomains: From model membranes to lymphocyte function, Prostaglandins Leukot. Essent. Fatty Acids 87 (6) (2012) 205–208, https://doi.org/10.1016/j.plefa.2012.09.007.
[22] J. Whelan, K.M. Gowdy, S.R. Shaikh, N-3 polyunsaturated fatty acids modulate B cell activity in pre-clinical models: Implications for the immune response to infections, Eur. J. Pharmacol. 785 (2016) 10–17, https://doi.org/10.1016/j.ejphar.2015.03.100.
[23] D. Cucchi, D. Camacho-Muñoz, M. Certo, J. Niven, J. Smith, A. Nicolaou, C. Mauro, Omega-3 polyunsaturated fatty acids impinge on CD4^{+} T cell motility and adipose tissue distribution via direct and lipid mediator-dependent effects, Cardiovasc. Res. 116 (5) (2019) 1006–1020, https://doi.org/10.1093/cvr/cvz208.
[24] Y.A. Hannun, L.M. Obeid, Sphingolipids and their metabolism in physiology and disease, Nat. Rev. Mol. Cell Biol. 19 (3) (2018) 175–191, https://doi.org/10.1038/nrm.2017.107.
[25] C.D. Green, M. Maceyka, L.A. Cowart, S. Spiegel, Sphingolipids in metabolic disease: The good, the bad, and the unknown, Cell Metab. 33 (7) (2021) 1293–1306, https://doi.org/10.1016/j.cmet.2021.06.006.
[26] B. Chaurasia, C.L. Talbot, S.A. Summers, Adipocyte Ceramides-The Nexus of Inflammation and Metabolic Disease, Front. Immunol. 11 (2020) 576347, https://doi.org/10.3389/fimmu.2020.576347.
[27] K.A. McGurk, B.D. Keavney, A. Nicolaou, Circulating ceramides as biomarkers of cardiovascular disease: Evidence from phenotypic and genomic studies, Atherosclerosis 327 (2021) 18–30, https://doi.org/10.1016/j.atherosclerosis.2021.04.021.
[28] K.A. McGurk, S.G. Williams, H. Guo, H. Watkins, M. Farrall, H.J. Cordell, A. Nicolaou, B.D. Keavney, Heritability and family-based GWAS analyses of the N-acyl ethanolamine and ceramide plasma lipidome, Hum. Mol. Genet. 30 (6) (2021) 500–513, https://doi.org/10.1093/hmg/ddab002.
[29] J.V. Varre, W.L. Holland, S.A. Summers, You aren't IMMUNE to the ceramides that accumulate in cardiometabolic disease, Biochim. Biophys. Acta Mol. Cell Biol. Lipids 1867 (6) (2022) 159125, https://doi.org/10.1016/j.bbalip.2022.159125.
[30] S. Schiffmann, D. Hartmann, S. Fuchs, K. Birod, N. Ferreiròs, Y. Schreiber, A. Zivkovic, G. Geisslinger, S. Grösch, H. Stark, Inhibitors of specific ceramide synthases, Biochimie 94 (2) (2012) 558–565, https://doi.org/10.1016/j.biochi.2011.09.007.
[31] D.C. Miller, K.B. Whittington, D.D. Brand, K.A. Hasty, E.F. Rosloniec, The CII-specific autoimmune T-cell response develops in the presence of FTY720 but is regulated by enhanced Treg cells that inhibit the development of autoimmune arthritis, Arthritis Res. Ther. 18 (1) (2016) 8, https://doi.org/10.1186/s13075-015-0909-6.
[32] A.M. Wolf, K. Eller, R. Zeiser, C. Dürr, U.V. Gerlach, M. Sixt, L. Markut, G. Gastl, A. R. Rosenkranz, D. Wolf, The sphingosine 1-phosphate receptor agonist FTY720 potently inhibits regulatory T cell proliferation in vitro and in vivo, J. Immunol. 183 (6) (2009) 3751–3760, https://doi.org/10.4049/jimmunol.0901011.
[33] A. Schmidt, S. Éliás, R.N. Joshi, J. Tegnér, In Vitro Differentiation of Human CD4^{+}FOXP3^{+} Induced Regulatory T Cells (iTregs) from Naïve CD4^{+} T Cells Using a TGF-β-containing Protocol, J. Vis. Exp. 118 (2016) e55015, https://doi.org/10.3791/55015.
[34] C.A. Schneider, W.S., Rasband, K.W., Eliceiri. NIH Image to ImageJ: 25 years of image analysis, Nature methods, 9 (2012) 671-675. DOI: 10.1038/NMETH.2089.
[35] D. Camacho-Muñoz, M. Kiezel-Tsugunova, O. Kiss, M. Uddin, M. Sundén, M. Ryaboshapkina, L. Lind, J. Oscarsson, A. Nicolaou, Omega-3 carboxylic acids and fenofibrate differentially alter plasma lipid mediators in patients with non-alcoholic fatty liver disease, FASEB J. 35 (11) (2021) e21976, https://doi.org/10.1096/fj.202100380RRR.
[36] A.C. Kendall, S.M. Pilkington, K.A. Massey, G. Sassano, L.E. Rhodes, A. Nicolaou, Distribution of Bioactive Lipid Mediators in Human Skin, J. Invest. Dermatol. 135 (6) (2015) 1510–1520, https://doi.org/10.1038/jid.2015.41.
[37] Y. Masukawa, H. Narita, E. Shimizu, N. Kondo, Y. Sugai, T. Oba, R. Homma, J. Ishikawa, Y. Takagi, T. Kitahara, Y. Takema, K. Kita, Characterization of overall ceramide species in human stratum corneum, J. Lipid Res. 49 (7) (2008) 1466–1476, https://doi.org/10.1194/jlr.M800014-JLR200.
[38] A.C. Kendall, M. Kiezel-Tsugunova, L.C. Brownbridge, J.L. Harwood, A. Nicolaou, Lipid functions in skin: Differential effects of n-3 polyunsaturated fatty acids on cutaneous ceramides, in a human skin organ culture model, Biochim. Biophys. Acta Biomembr. 1859(9 Pt B) (2017) 1679-1689. DOI: 10.1016/j.bbamem.2017.03.016.
[39] J.-W. Park, W.-J. Park, A.H. Futerman, Ceramide synthases as potential targets for therapeutic intervention in human diseases, Biochim. Biophys. Acta 1841 (5) (2014) 671–681, https://doi.org/10.1016/j.bbalip.2013.08.019.
[40] C. Mauro, J. Smith, D. Cucchi, D. Coe, H. Fu, F. Bonacina, A. Baragetti, G. Cermenati, D. Caruso, N. Mitro, A.L. Catapano, E. Ammirati, M.P. Longhi, K. Okkenhaug, G.D. Norata, F.M. Marelli-Berg, Obesity-Induced Metabolic Stress Leads to Biased Effector Memory CD4+ T Cell Differentiation via PI3K p110δ-Akt-

Mediated Signals, Cell Metab. 25 (3) (2017) 593–609, https://doi.org/10.1016/j.cmet.2017.01.008.
[41] E.L. Laviad, L. Albee, I. Pankova-Kholmyansky, S. Epstein, H. Park, A.H. Merrill, A. H. Futerman, Characterization of Ceramide Synthase 2: tissue distribution, substrate specificity, and inhibition by sphingosine 1-phosphate, J. Biol. Chem. 283 (9) (2008) 5677–5684, https://doi.org/10.1074/jbc.M707386200.
[42] E.V. Berdyshev, I. Gorshkova, A. Skobeleva, R. Bittman, X. Lu, S.M. Dudek, T. Mirzapoiazova, J.G.N. Garcia, V. Natarajan, FTY720 Inhibits Ceramide Synthases and Up-regulates Dihydrosphingosine 1-Phosphate Formation in Human Lung Endothelial Cells, J. Biol. Chem. 284 (9) (2009) 5467–5477, https://doi.org/10.1074/jbc.M805186200.
[43] L. Liu, X. Cheng, H. Yang, S. Lian, Y. Jiang, J. Liang, X. Chen, S. Mo, Y. Shi, S. Zhao, J. Li, R. Jiang, D.H. Yang, Y. Wu, BCL-2 expression promotes immunosuppression in chronic lymphocytic leukemia by enhancing regulatory T cell differentiation and cytotoxic T cell exhaustion, Mol. Cancer 21 (1) (2022) 59, https://doi.org/10.1186/s12943-022-01516-w.
[44] J.P. Snook, C. Kim, M.A. Williams, TCR signal strength controls the differentiation of $CD4^+$ effector and memory T cells, Sci. Immunol. 3 (25) (2018) eass9103, https://doi.org/10.1126/sciimmunol.aas9103.
[45] J.F. Lim, H. Berger, I.H. Su, Isolation and Activation of Murine Lymphocytes, J. Vis. Exp. 116 (2016) e54596, https://doi.org/10.3791/54596.
[46] B.D. McNally, D.F. Ashley, L. Hänschke, H.N. Daou, N.T. Watt, S.A. Murfitt, A.D. V. MacCannell, A. Whitehead, T.S. Bowen, F.W.B. Sanders, M. Vacca, K.K. Witte, G. R. Davies, R. Bauer, J.L. Griffin, L.D. Roberts, Long-chain ceramides are cell non-autonomous signals linking lipotoxicity to endoplasmic reticulum stress in skeletal muscle, Nat. Commun. 13 (1) (2022) 1748, https://doi.org/10.1038/s41467-022-29363-9.
[47] C. Walchuk, Y. Wang, M. Suh, The impact of EPA and DHA on ceramide lipotoxicity in the metabolic syndrome, Br. J. Nutr. 125 (8) (2021) 863–875, https://doi.org/10.1017/S0007114520003177.
[48] C. Shah, G. Yang, I. Lee, J. Bielawski, Y.A. Hannun, F. Samad, Protection from High Fat Diet-induced Increase in Ceramide in Mice Lacking Plasminogen Activator Inhibitor 1, J. Biol. Chem. 283 (20) (2008) 13538–13548, https://doi.org/10.1074/jbc.M709950200.
[49] S. Raichur, B. Brunner, M. Bielohuby, G. Hansen, A. Pfenninger, B. Wang, J. C. Bruning, P.J. Larsen, N. Tennagels, The role of C16:0 ceramide in the development of obesity and type 2 diabetes: CerS6 inhibition as a novel therapeutic approach, Mol. Metab. 21 (2019) 36–50, https://doi.org/10.1016/j.molmet.2018.12.008.
[50] N. Turner, X.Y. Lim, H.D. Toop, B. Osborne, A.E. Brandon, E.N. Taylor, C. E. Fiveash, H. Govindaraju, J.D. Teo, H.P. McEwen, T.A. Couttas, S.M. Butler, A. Das, G.M. Kowalski, C.R. Bruce, K.L. Hoehn, T. Fath, C. Schmitz-Peiffer, G. J. Cooney, M.K. Montgomery, J.C. Morris, A.S. Don, A selective inhibitor of ceramide synthase 1 reveals a novel role in fat metabolism, Nat. Comm. 9 (1) (2018) 3165, https://doi.org/10.1038/s41467-018-05613-7.
[51] S. Raichur, S.T. Wang, P.W. Chan, Y. Li, J. Ching, B. Chaurasia, S. Dogra, M. K. Öhman, K. Takeda, S. Sugii, Y. Pewzner-Jung, A.H. Futerman, S.A. Summers, CerS2 Haploinsufficiency Inhibits β-Oxidation and Confers Susceptibility to Diet-Induced Steatohepatitis and Insulin Resistance, Cell Metab 20 (4) (2014) 687–695, https://doi.org/10.1016/j.cmet.2014.09.015.
[52] D. Gosejacob, P.S. Jäger, K. vom Dorp, M. Frejno, A.C. Carstensen, M. Köhnke, J. Degen, P. Dörmann, M. Hoch, Ceramide Synthase 5 Is Essential to Maintain C16:0-Ceramide Pools and Contributes to the Development of Diet-induced Obesity, J. Biol. Chem. 291 (13) (2016) 6989–7003, https://doi.org/10.1074/jbc.M115.691212.
[53] S.M. Turpin, H.T. Nicholls, D.M. Willmes, A. Mourier, S. Brodesser, C. M. Wunderlich, J. Mauer, E. Xu, P. Hammerschmidt, H.S. Brönneke, A. Trifunovic, G. LoSasso, F.T. Wunderlich, J.-W. Kornfeld, M. Blüher, M. Krönke, J.C. Brüning, Obesity-Induced CerS6-Dependent C16:0 Ceramide Production Promotes Weight Gain and Glucose Intolerance, Cell Metabol. 20 (4) (2014) 678–686, https://doi.org/10.1016/j.cmet.2014.08.002.
[54] S.-H. Shin, K.-A. Cho, H.-S. Yoon, S.-Y. Kim, H.-Y. Kim, Y. Pewzner-Jung, S.-A. Jung, W.-J. Park, A.H. Futerman, J.-W. Park, Ceramide Synthase 2 Null Mice Are Protected from Ovalbumin-Induced Asthma with Higher T Cell Receptor Signal Strength in $CD4^+$ T Cells, Int. J. Mol. Sci. 22 (5) (2021) 2713, https://doi.org/10.3390/ijms22052713.
[55] T. Wiese, F. Dennstädt, C. Hollmann, S. Stonawski, C. Wurst, J. Fink, E. Gorte, P. Mandasari, K. Domschke, L. Hommers, B. Vanhove, F. Schumacher, B. Kleuser, J. Seibel, J. Rohr, M. Buttmann, A. Menke, J. Schneider-Schaulies, N. Beyersdorf, Inhibition of acid sphingomyelinase increases regulatory T cells in humans, Brain Commun. 3 (2) (2021), https://doi.org/10.1093/braincomms/fcab020.
[56] Y.H. Chen, S. Lightman, V.L. Calder, $CD4^+$ T-Cell Plasticity in Non-Infectious Retinal Inflammatory Disease, Int. J. Mol. Sci. 22 (17) (2021) 9584, https://doi.org/10.3390/ijms22179584.
[57] P. Sen, S.B.A. Andrabi, T. Buchacher, M.M. Khan, U.U. Kalim, T.M. Lindeman, M. A. Alves, V. Hinkkanen, E. Kemppainen, A.M. Dickens, O. Rasool, T. Hyötyläinen, R. Lahesmaa, M. Orešič, Quantitative genome-scale metabolic modeling of human $CD4^+$ T cell differentiation reveals subset-specific regulation of glycosphingolipid pathways, Cell Rep. 37 (6) (2021) 109973, https://doi.org/10.1016/j.celrep.2021.109973.
[58] M.O. Li, A.Y. Rudensky, T cell receptor signalling in the control of regulatory T cell differentiation and function, Nat. Rev. Immunol. 16 (4) (2016) 220–233, https://doi.org/10.1038/nri.2016.26.
[59] A.H. Courtney, W.L. Lo, A. Weiss, T.C.R. Signaling, Mechanisms of Initiation and Propagation, Trends Biochem. Sci. 43 (2) (2018) 108–123, https://doi.org/10.1016/j.tibs.2017.11.008.
[60] F. Lachkar, P. Ferré, F. Foufelle, A. Papaioannou, Dihydroceramides: their emerging physiological roles and functions in cancer and metabolic diseases, Am. J. Physiol. Endocrinol. Metabol. 320 (1) (2021) E122–E130, https://doi.org/10.1152/ajpendo.00330.2020.